Journal of Petroleum Science and Engineering 78 (2011) 288–303

Contents lists available at ScienceDirect

Journal of Petroleum Science and Engineering

journal homepage: www.elsevier.com/locate/petrol

Taking advantage of injectivity decline for improved recovery during waterflood with horizontal wells

Pavel G. Bedrikovetsky [a,*], Thi K.P. Nguyen [a], Andrew Hage [a], John R. Ciccarelli [a], Mohammad ab Wahab [a], Gladys Chang [b], Antonio Luiz S. de Souza [c], Claudio A. Furtado [c]

[a] University of Adelaide, Australian School of Petroleum, North Terrace, Santos Petroleum Engineering Blg, Adelaide, SA 5005, Australia
[b] Schlumberger, Australia
[c] Petrobras, Brazil

ARTICLE INFO

Article history:
Received 3 November 2009
Accepted 23 May 2011
Available online xxxx

Keywords:
Injectivity
Raw water
PWRI
Waterflooding
Sweep efficiency
Waterflood simulation

ABSTRACT

Injectivity formation damage with waterflooding using sea/produced water has been widely reported in the North Sea, the Gulf of Mexico and the Campos Basin in Brazil. The damage is due to the capture of solid and/or liquid particles by reservoir rock that consequently leads to the permeability decline. Another reason for the permeability decline is the formation of a low permeable external filter cake.

However, moderate injectivity decline is not too damaging for a waterflood project with long horizontal injectors, where the initial injectivity index is high. In this case, the injection of raw or poorly treated water may significantly reduce the cost of water treatment, which is a cumbersome and expensive procedure in offshore projects.

In this paper we investigate the effects of injected water quality on waterflooding using horizontal wells. An analytical model for injectivity decline, which accounts for particle capture and a low permeable external filter cake formation, has been implemented into black oil reservoir simulator. It was found that induced injectivity damage results in a noticeable reduction of water cut and in increased (although delayed) sweep efficiency.

1. Introduction

Injectivity decline is a widely spread phenomenon in waterflood projects. Usually it occurs due to the injected water containing solid and liquid particles. Particle capture by the rock decreases the permeability and the formation of an external filter cake on the well surface increases the hydraulic resistivity of the system (Pang and Sharma, 1997; Ochi et al., 1999; Al-Abduwani et al., 2005a). Both phenomena result in the decline of well index. The injectivity decline occurs during seawater injection, re-injection of produced water (PWRI) and injection of any poor quality water (Nabzar et al., 1996, 1997; Chauveteau et al., 1998; Rousseau et al., 2007).

The injectivity damage can be prevented or mitigated by injected water treatment, which is an extremely expensive operation under offshore conditions. Water treatment costs remain high even with the relocation of treatment facilities onto the sea floor. The subject of cost reduction for injected water treatment is becoming of extreme importance worldwide due to increasing oil production by waterflooding, especially from offshore deep-water oil fields.

The formation damage, induced by the captured particles and filter cake, leads to the homogenisation of the injectivity profile (Khambharatana et al., 1997, 1998) and decreases residual oil saturation (Soo and Radke, 1986a,b). Yet, it was found that the particle retention phenomena take place within a close vicinity of injection wells. In the case of vertical injectors used in thin layer-cake reservoir, the injected water bypasses the damaged zone near to the vertical injector by moving vertically along a short distance from low permeability to high permeability layer. The perturbation of the stream line system due to the induced formation damage is minimal. So, the un-uniformly distributed skin, induced along the vertical well, almost do not affect the oil-water flow away from the injector. Therefore, the injectivity profile homogenization has a little effect on sweep efficiency for the case of vertical wells in layer-cake reservoirs. For long horizontal wells, where the well length have the same order of magnitude as the inter-well distance, it would take much longer for water to bypass the damaged zone by moving "parallel" to the injector in order to enter the faster flow path. So, it is expected that the injectivity profile homogenization may result in more significant sweep increase in a

* Corresponding author. Tel.: +61 883033082.
E-mail address: pavel.russia@gmail.com (P.G. Bedrikovetsky).

0920-4105/$ – see front matter © 2011 Elsevier B.V. All rights reserved.
doi:10.1016/j.petrol.2011.05.020

system of long horizontal wells. Nevertheless, the corresponding studies are not available in the literature.

The effects of near-well formation damage on waterflood performance have long been recognised (Civan, 2007). Skin factor in injection wells grows with time due to reservoir clogging and cake formation (Pang and Sharma, 1997; Wennberg and Sharma, 1997; Mojarad and Settari, 2007). Despite this, to the best of our knowledge, the formation damage options in modern reservoir simulators are designed for a constant skin factor throughout the field life.

In the current paper we investigate the effects of injectivity skin in a system of horizontal wells, induced from the injection of poorly treated water, in order to create incremental oil recovery. The waterflood black-oil reservoir simulator (ECLIPSE 100) was coupled with the analytical model for injectivity decline (Pang and Sharma, 1997; Wennberg and Sharma, 1997; Ochi et al., 1999; Bedrikovetsky et al., 2005; Paiva et al., 2007). The simulation results show the noticeable effect of injectivity decline provoked by the injection of poor quality water on the water cut history and the reservoir sweep by waterflooding.

The structure of the paper is as follows. Firstly, the reservoir physical factors leading to incremental recovery due to low quality water injection are discussed. Then, we describe the analytical model for injectivity index decline due to deep bed filtration of injected particles and low permeable external cake formation. Finally, the implementation of the analytical model into the black-oil ECLIPSE 100 reservoir simulator is discussed followed by the results of waterflood modelling.

2. Reservoir physics of interaction between the injectivity and waterflooding

Let us discuss why the injection of water with particles induces formation damage that may result in sweep efficiency increase and in reduction of the amount of injected water.

Heterogeneity of oil bearing formations is a major factor controlling the oil recovery during waterflooding. Water enters mostly in high permeability zones. The breakthrough of low viscosity water fingers forms a high conductivity channel between the injection and production wells. This leads to the 'recirculation' of a significant fraction of injected water without further displacement of any significant oil volumes.

Several Enhanced Oil Recovery (EOR) methods are based on the plugging of swept areas and redirection of the injected water into unswept zones (Lake, 1989; Bedrikovetsky, 1993). The possibility of poor quality water injection, where the particles are captured by the rock causing the permeability decrease in the waterflooded zones and the consequent sweep increase, has been discussed in the literature (Khambharatana et al., 1997, 1998). The particles, which are captured in pores where water has already entered, decrease the amount of residual oil (Soo and Radke, 1986a, b). These phenomena encouraged the considerations of the injection of particulated water for improved oil recovery. The mass of retained particles is a monotonically increasing function of injected water volume (Herzig et al., 1970). So, the induced skin is high 'in front' of high permeability zones or 'at the beginning' of high-velocity streamlines. The possibility of preferential plugging of swept zones by the 'captured' particles was discussed for vertical injectors (Khambharatana et al., 1997, 1998). Yet, it was found that the injectivity damage is induced by the particles which are captured near to injection wells; the damaged zone radius rarely exceeds 1–2 m (Nunes et al., 2010). So, the injected water by-passes the damaged zone and enters the highly permeable zone or the high-velocity stream lines close to the injector. Therefore, the incremental sweep efficiency due to the induced formation damage is small and the reservoir simulations show a negligible sweep increase due to the induced injectivity damage in system of vertical wells.

Let us consider the application of poorly treated water in reservoirs with long horizontal injectors for both horizontal and vertical producers. Preferential deposition of particles 'in front' of the high-speed streamlines causes an increase of 'flight' times. High variation of streamline sizes and speeds for long horizontal wells may result in the preferential plugging of highly swept zones and in the significant increase of sweep efficiency.

Fig. 1 shows a displacement schematic in a horizontal two-permeability-zone reservoir with two horizontal wells. Water enters preferably in the high permeability zone. Therefore, the main portion of the injected water passes via the well sections in the highly permeable zone. So, the particles deposit mainly in the highly permeable zone which then creates an additional resistance to the flow of water. It slows down the displacement front in the high permeability zone and delays the water breakthrough. The continuous line in Fig. 1 corresponds to the reservoir sweep by 'clean' water in a damage-free case. The injected suspension is redirected into the low permeability zone resulting in increased reservoir sweep.

The final conclusion of the importance of the sweep increase effect must be based on results of reservoir simulations that account for injectivity damage.

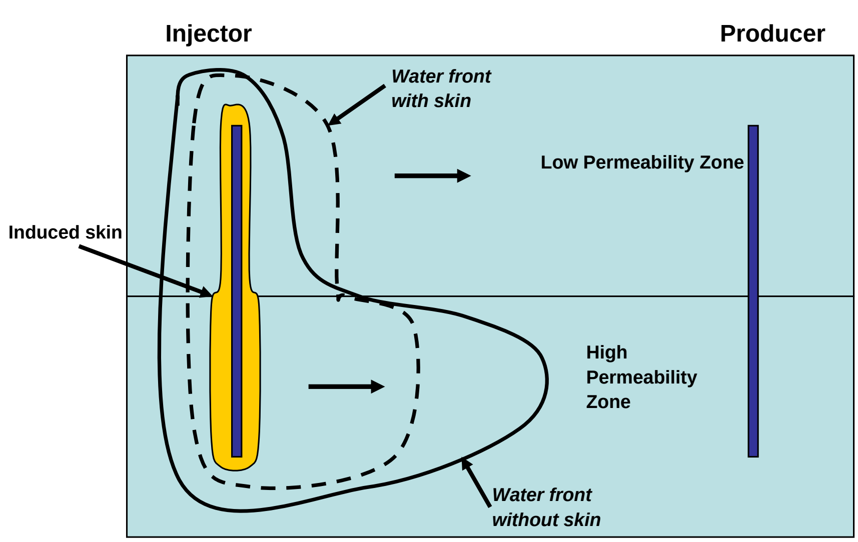

Fig. 1. Schematic for improved sweep of low permeability zone due to skin, induced by injectivity of low quality water, in a two-permeability-zone reservoir.

3. Analytical model for injectivity damage due to injection of poor quality water

Let us consider an analytical model for injectivity decline during injection of particle suspension for further implementation into a waterflooding reservoir simulator.

The mathematical macro scale model for one-phase flow of particulated water includes equations of mass conservation law for suspended and retained particles and of particle capture kinetics (Herzig et al., 1970; Pang and Sharma, 1997). The model operates with overall suspended and retained concentrations and does not consider pore and particle radii distributions. Different pore scale micro models with various mechanisms of particle transport and retention (Sharma and Yortsos, 1987; Bedrikovetsky, 2008; Shapiro and Bedrikovetsky, 2008) result in the same macro scale model that is presently used for formation damage prediction.

Generally speaking, the mathematical model for displacement of oil by water with particles includes equations of mass balance for suspended and retained particles and of particle capture kinetics in addition to the black-oil-model equations of mass balance for oil and water (Aziz and Settari, 2002). Therefore, the injectivity damage effects during waterflooding using raw water cannot be captured by standard black-oil models.

Nevertheless, the black-oil and injectivity decline models can be coupled in the same reservoir simulator. Despite the deep propagation of injected particles into the formation and some particle retention far away from the injector, the injection well index is reduced mainly by the particles which are deposited near to the wellbore (Nunes et al., 2010). Thus, it allows the consideration of the retention of injected particles near to the well only, by calculating the dynamics of skin factor and including the growing skin into the well boundary condition.

There are three stages of the injectivity damage process:

(1) Deep bed filtration, where particles penetrate into the formation (Herzig et al., 1970; Ali et al., 2005; Ali and Currie, 2007);
(2) Building up the low permeability external filter cake (Pang and Sharma, 1997; Ochi et al., 1999);
(3) Particle dislodging from the cake surface by the drag force exerting the particles by the downward flowing water (Jiao and Sharma, 1994; Freitas and Sharma, 2001; Al-Abduwani et al., 2005b).

Fig. 2 presents particle retention in the pore space. When the rock inlet is sufficiently filled by the retained particles so that no more of them can enter, the particles accumulate upstream of the rock entrance and form an external filter cake.

The particle dislodging from the filter cake surface occurs if the total of drag and lifting force moments, acting on the particle, exceeds the electrostatic force moment. After this occurrence, no further particles are retained on the filter cake surface, and the injectivity index remains constant.

Fig. 3 presents the plot of reciprocal to the normalised well index (so called impedance) versus dimensionless time t_D as being measured in the injected pore volumes

$$j(t_D)=\frac{q_0}{q(t_D)}\frac{\Delta p(t_D)}{\Delta p_0} \tag{1}$$

Here q is the injection rate, Δp is the pressure drawdown and subscript “0” corresponds to the beginning of injection.

The curve is piece-wise-linear during both deep bed filtration and external filter cake formation and reaches the plateau during filter cake erosion. Recalculating well impedance (reciprocal to normalised well index in Eq. (1)) into skin factor S

$$j(t_D)=\frac{\ln {r_e}/{r_w}+S}{\ln {r_e}/{r_w}} \tag{2}$$

yields:

$$S(t_D)=\begin{cases}\ln {r_e}/{r_w}\, m t_D, & 0<t_D<t_{Dtr}\\ \ln {r_e}/{r_w}\,(m t_{Dtr}+m_c(t_D-t_{Dtr})), & t_{Dtr}<t_D<t_{De}\\ \ln {r_e}/{r_w}\,(m t_{Dtr}+m_c(t_{De}-t_{Dtr})), & t_{De}<t_D\end{cases} \tag{3}$$

Here r_e and r_w are the drainage and well radii, respectively, m is so-called impedance growth coefficient, t_{Dtr} and t_{De} are dimensionless transition and erosion times, respectively. The tangent m is defined by the filtration coefficient λ', formation damage coefficient β, porosity ϕ and injected particle concentration c^0. The tangent m_c is defined by the cake permeability k_c, cake porosity ϕ_c, initial rock permeability k_0 and porosity ϕ. The corresponding formulae are presented in Bedrikovetsky et al. (2005) and Paiva et al. (2007).

The definitions of parameters can be found in Herzig et al. (1970) and Pang and Sharma (1997). The brief derivations and final expressions for skin factor are presented in Appendix A, B. The analytical model for injectivity index decline during suspension/colloid injection allows implementing the injectivity damage model into skin factor option of the black-oil model (Schlumberger, 2008).

4. Implementation of injectivity decline into black oil reservoir simulator

Let us discuss a simplified waterflooding reservoir model in order to separate effects of the un-uniformly distributed induced skin from

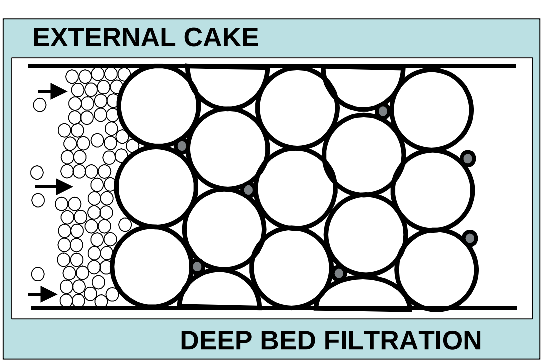

Fig. 2. Schematic for injectivity damage during deep bed filtration, external filter cake formation and cake erosion.

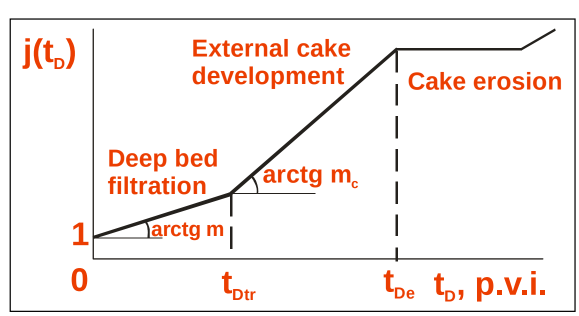

Fig. 3. Increase of reciprocal injectivity index during deep bed filtration, external filter cake formation and cake erosion.

other physics phenomena, which could also affect the waterflood oil recovery. It is assumed that the pressure on injection well is a given function of time, which does not exceed the fractured pressure value. It allows avoiding the complex effects of fracturing and the injectivity damage induced by leak-off on waterflood performance (Hoek van den, 2004; Ojukwu and Hoek van den, 2004; Das et al., 2009; Izgec and Kabir, 2009). Pressure redistribution due to the injectivity decline may cause a significant rock deformation. So, it is also assumed that the rock deformation is negligible and the coupled flow-geo-mechanics phenomena (Mojarad and Settari, 2007) can be avoided (see Furtado et al., 2007 about the application of PETEX's simulator REVEAL to capture geo-mechanics effects on well injectivity). Water is injected at the reservoir temperature, so the effects of changing water viscosity on injectivity (Bennion et al., 1996) and relative permeability (Lake, 1989) are not accounted for.

The Peaceman's boundary condition on a well accounting for skin factor is based on steady state water flow from the injector into the reservoir (Aziz and Settari, 2002)

$$q = 2\pi r_e h \frac{k k_{rwor}}{\mu_w} \frac{\partial p}{\partial r}\bigg|_{r=r_e} = \frac{2\pi k k_{rwor} h}{\mu_w} \frac{p_w - p_e}{\ln {r_c}/{r_w} + S(t_D)} \tag{4}$$

Here h is the thickness of the reservoir, k is the absolute permeability of water, k_{rwor} is the relative permeability of water to residual oil, μ_w is water viscosity, p_w is the well pressure and p_e is the average reservoir pressure.

In the case of long horizontal wells, boundary conditions Eq. (4) are applied separately for each well section. It is assumed that the pressure losses along the injection and production wells are negligibly small if compared with the pressure drawdown across the reservoir, so constant pressures have been fixed on both wells.

The Eclipse option of waterflooding with skin factor requires setting the skin factor value at every time step (see Schlumberger, 2008). Let us consider the case of given bottomhole pressures as boundary conditions on wellbore walls. Initially, the injection rate distribution along the well in each well section is calculated. This allows calculating the skin induced by the first time step using formula in Eq. (3). Since the rate is not constant along the well, the skin is also not constant. The second equality Eq. (4) provides the well boundary condition; it allows us to perform the finite difference calculations and to obtain a new rate distribution along the well, resulting in a new average reservoir pressure p_e. It results in skin re-calculation for each well section by Eq. (3) and in a new boundary condition Eq. (4) for the second time step, as well as for all subsequent time steps.

The values of skin factor obtained from Eq. (3) were exported into the black-oil reservoir simulator ECLIPSE 100 under the keyword COMPDAT. A time step of 90 days was used for the model in order to represent skin build-up in the reservoir during raw water injection.

So, the skin factor is updated at each time step according to varying injection rate following simulation of well rate and pressure in the neighbouring cell points.

5. Results of reservoir simulation

In this section, the reservoir simulator ECLIPSE 100 with implemented formation damage model in Eq. (3) has been used to analyse the effects of induced injectivity formation damage on waterflooding in three different cases of horizontal well placing.

5.1. Parallel horizontal injector and producer in thin horizontal reservoir with high and low permeability zones

The exploitation of a thin horizontal reservoir with lateral low permeability and high permeability zones and without vertical heterogeneity completed with two parallel injection and production wells was simulated (Fig. 1). It is assumed that the well pressures are above bubble point pressure during the overall injection-production period, i.e. two-phase flow of immiscible fluids takes place.

The injection and production pressures are imposed on the wells ($r = r_w$) as boundary conditions, i.e. the distribution of rates along wells are calculated by the simulations. The permeabilities of the two zones are 50 and 500 md. The default values for relative permeability and capillary pressure have been used. Both well lengths were 200 m. Oil viscosity was 1 cp. The main grid and reservoir parameters are presented in Table 1.

The data for analytical modelling of injectivity damage are presented in Tables 2, where the usual range values of formation damage parameters were taken (Pang and Sharma, 1997; Wennberg and Sharma, 1997; Bedrikovetsky et al., 2001; Moghadasi et al., 2004). Let us compare waterflood sweep with injection of clean water and poor quality water, which results in $S = 60$ after 1 PVI. This high number is acceptable at deep water offshore waterflood projects. Souza et al., 2005, reports about 10-times injectivity decrease in giant field A (Brazil, Campos Basin), which corresponds to skin factor $S = 83$ for well radius $r_w = 0.1$ m and well drainage radius $r_e = 1000$ m. Furui et al., 2003, considers skin factor up to 30–40. Bennion et al., 1996, calls skin factor up to 10 as the “low skin regime”. The authors investigate “S until 200, … which may occur in a badly damaged overbalanced open-hole completion”. The plots and dependencies in this paper are presented until $S = 200$.

Fig. 4a,b present saturation fields after 1 PVI for the cases with and without skin, respectively. Fast breakthrough and low sweep took place for the case with no skin. It is seen that the sweep is higher in the high permeability zone. The bulk of water enters the high permeability zone; therefore resulting in the higher induced skin around the part of well in this zone as skin is a monotonically increasing function of the volume of injected water (Fig. 3). The increased skin along the sections of the horizontal well located in highly permeable zone yields

Table 1
Parameters used for the simulated models.

Parameters of the reservoir model	Two-zone reservoir	Bottom-up flooding
Numbers of nodes for fine grids	100×100×1	–
Numbers of nodes for moderate grids	50×50×1	50×50×3
Numbers of nodes for coarse grids	25×25×1	–
The length of the reservoir (m)	1000	500
The width of the reservoir (m)	1000	500
The thickness of the reservoir (m)	10	30
The length of wells (m)	200/320	200
Initial reservoir pressure (psi)	3000	3000
Viscosity of water (cp)	1	1
Viscosity of oil (cp)	1	1
Initial oil saturation	0.9	0.9
Initial porosity	0.3	0.3
Horizontal permeability (md)	50 & 500	50
Vertical permeability (md)	10	10
Producer bottom hole pressure (psi)	2500	2500
Injection pressure (psi)	5000	5000

Table 2
Data for simulation of waterflooding in the two-zone reservoir.

Data	S = 11	S = 25	S = 40	S = 60
λ' (1/m)	1	1	1	1
α	0.2	0.2	0.2	0.2
β	150	250	300	500
ϕ	0.3	0.3	0.3	0.3
c^0 (ppm)	5	10	15	25
r_w (m)	0.14	0.14	0.14	0.14
k_c (md)	20	20	20	20
ϕ_c	0.2	0.2	0.2	0.2

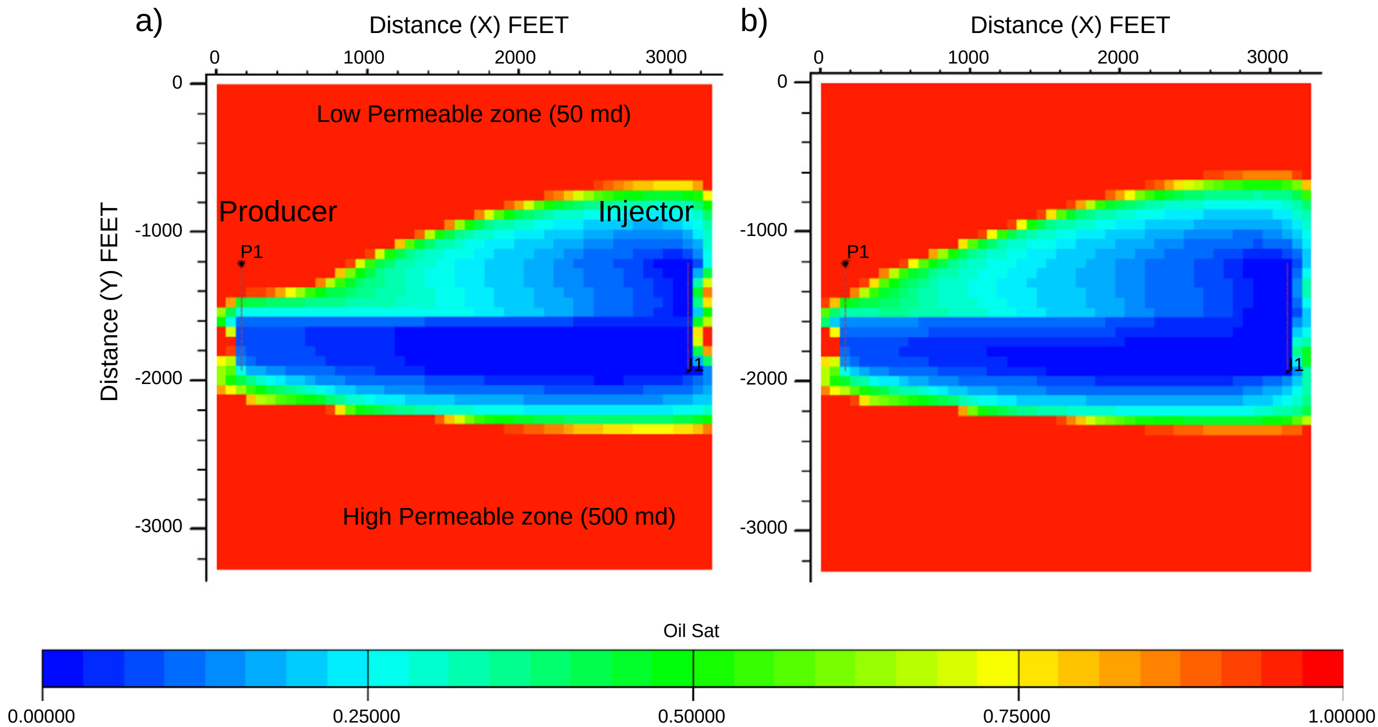

Fig. 4. Improved sweep efficiency with injectivity damage after 1 PVI for "short" horizontal wells. a) Sweep efficiency with no damage after 1 PVI. b) Sweep efficiency with high damage (S = 60) after 1 PVI.

the reduction of invaded water in this zone (Fig. 1). Automatically, the difference of fluxes is redirected into the low permeable zone, resulting in its better sweep. Fig. 4b shows increased water saturation in the low permeability zone if compared with Fig. 4a.

Homogenisation of the injectivity profile by induced skin also results in better sweep behind the injector. Fig. 4a shows some oil trapped near to the zone boundary. Two water fluxes in different permeability zones reach the boundary behind the injector at different times and start moving in opposite directions, resulting in trapped oil behind the injector. Induced skin leads to a decrease of time difference of front arrival to the impermeable boundary, which results in some decrease of trapped oil.

The effect of the induced injectivity skin, non-uniformly distributed along horizontal well, on the recovery factor *vs* injected volume of water is presented in Fig. 5 for three cases of volatile, conventional and heavy oils. The damage-free injection of clean water is considered along with injection of four poor quality waters resulting in different injectivity impairment. The injectivity damage parameters for four

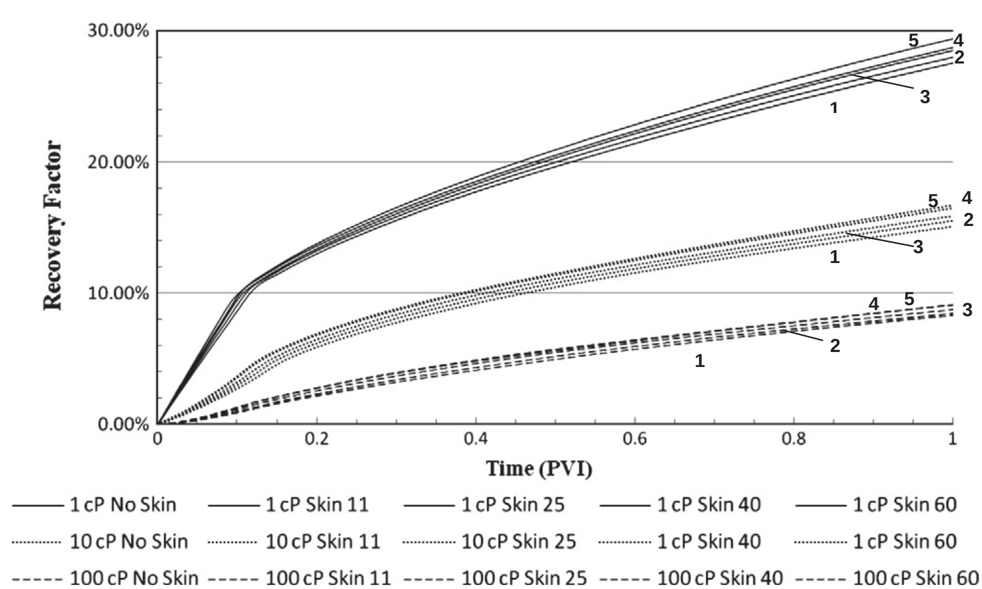

Fig. 5. Recovery factor versus time (PVI) for injection of suspension and of "clean" water. Curves 1, 2, 3, 4 and 5 correspond to injection of clean water and of suspensions resulting in skin factors 11, 25, 40 and 60 after 1 PVI, respectively. Solid, dotted and dashed curves correspond to oil viscosities 1 cp, 10 cp and 100 cp, respectively.

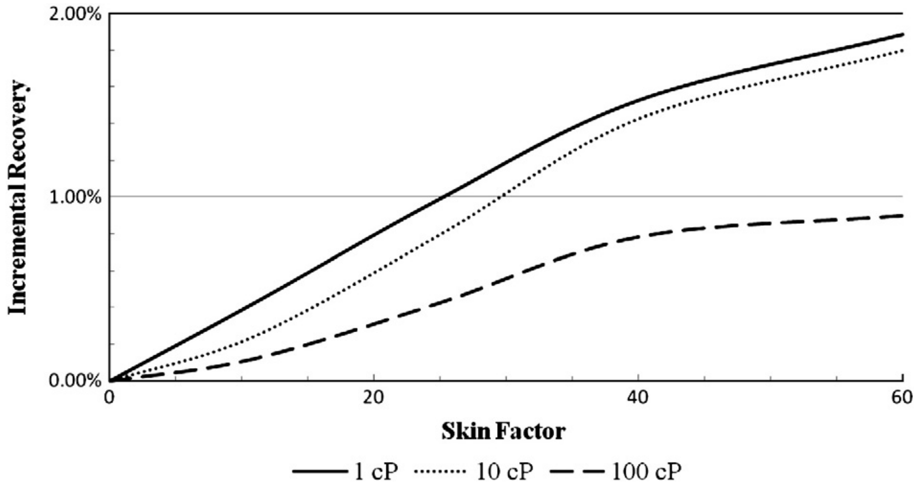

Fig. 6. Incremental recovery by using suspension instead of clean water, versus skin factor (both are calculated after 1 PVI). Solid, dotted and dashed curves correspond to oil viscosities 1 cp, 10 cp and 100 cp, respectively.

cases are presented in Table 2. For all oil viscosities, the higher is the skin the higher is the incremental recovery factor after 1 PVI. If compared with clean water flooding, injection of particulate suspension into volatile oil reservoir yielding S = 60 after 1 PVI causes 1.8% of incremental recovery. The effect is less pronounced for higher viscosity oils – incremental recovery of 0.8% for 100 cp oil after 1 PVI (Fig. 6).

Despite the decreasing of incremental recovery with increasing oil viscosity, the relative effect of non-uniform distribution of the induced injectivity skin along horizontal well does not decrease since the recovery is lower for heavy oils. For the case of high skin S = 60 presented in Fig. 6, the incremental recovery factors for oil viscosities 1, 10 and 100 cp are 1.88%, 1.43% and 0.9%, respectively, while the absolute recovery factors are 29.09%, 16.63% and 8.98%. So, the ratios of the incremental recovery and the recovery factor (relative incremental recoveries) are 0.065, 0.086 and 0.1, respectively. Thus, the relative incremental recovery is the highest for heavy oils.

Along with the positive effect of sweep efficiency increase due to injectivity profile homogenisation, the induced skin yields the negative effect of flux and total rate reduction (the total rate is the sum of those for produced oil and water). Fig. 7 exhibits recovery factor versus real time for three different viscosity oils during injection of clean water along with injection of four different quality waters. The higher is the skin the lower is the recovery factor. Yet, the difference between the recovery curves is negligible. For volatile oil reservoir, the recovery factor for clean waterflooding after 10 years is 35.37% while for S = 60 it is lower at 34.25%. Finally, the negative effect of rate decrease is compensated by the positive effect of sweep increase.

As it follows from Fig. 7, the amount of produced oil versus real time is almost independent of the induced skin. Therefore, the

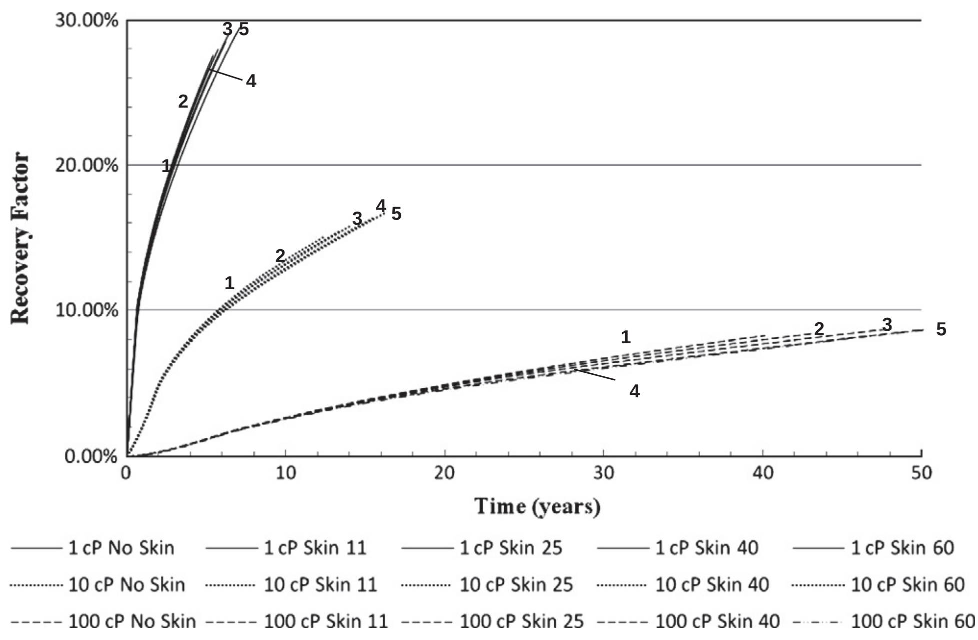

Fig. 7. Recovery factor versus real time for injection of clean water and of suspension. Curves 1, 2, 3, 4 and 5 correspond to injection of clean water and of suspensions resulting in skin factors of 11, 25, 40, 60 after 1 PVI, respectively. Solid, dotted and dashed curves correspond to oil viscosities 1 cp, 10 cp and 100 cp, respectively.

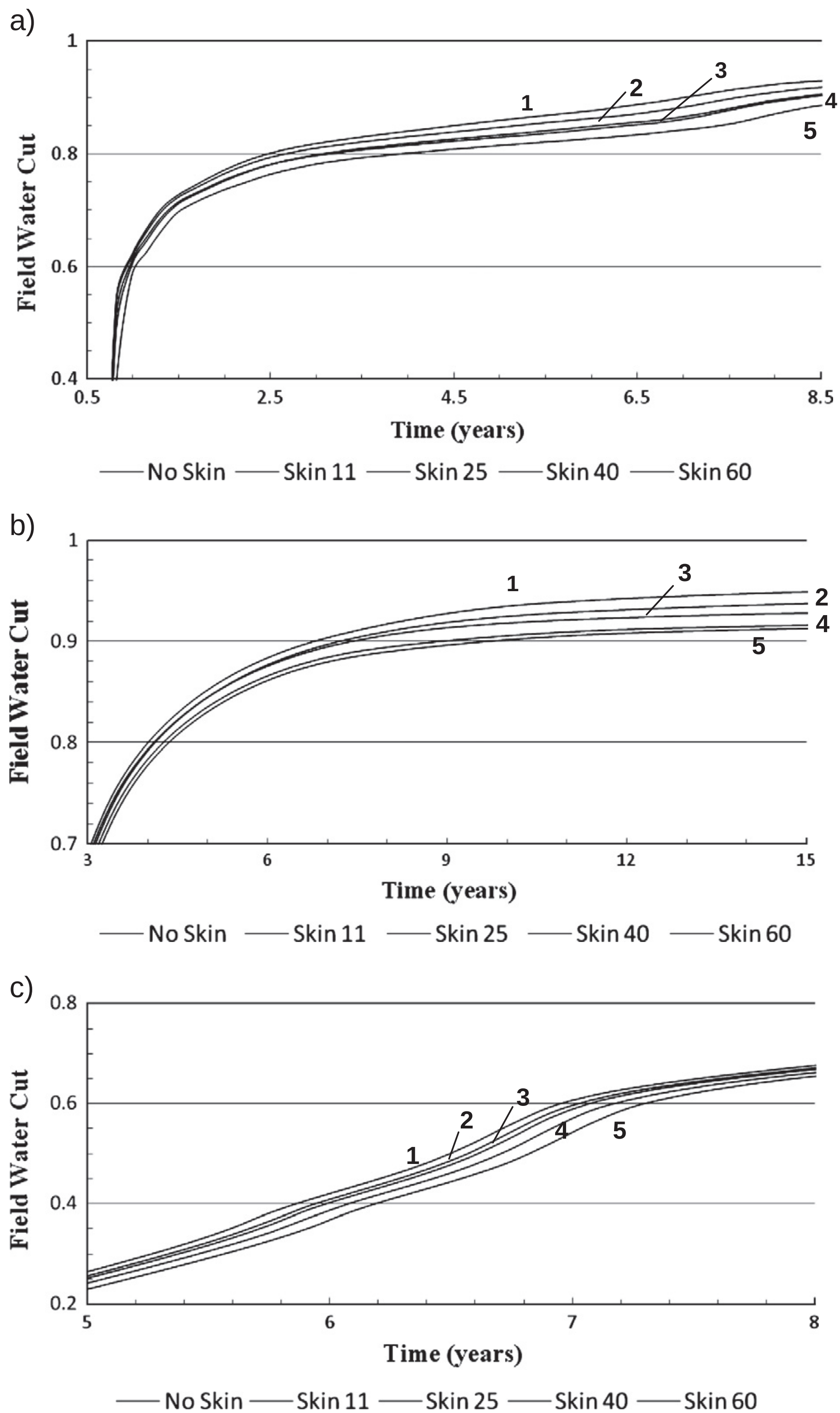

Fig. 8. Water cut during injection of suspension and of clean water, versus real time. Curves 1, 2, 3, 4 and 5 correspond to injection of clean water and of suspensions and skin factors 11, 25, 40 and 60 after 1 PVI, respectively. a) Oil viscosity is 1 cp, b) Oil viscosity is 10 cp, c) Oil viscosity is 100 cp.

comparison between the recovery efficiency indicators at the same production time means “at the same amount of produced oil”.

Fig. 8 shows how the water cut curve depends on the value of the induced skin. Fig. 8a-c show the water cut curves for volatile, conventional and heavy oils, respectively. The higher is the induced skin the lower is the water cut. For waterflooding in the volatile oil field, water cut reduction increases from 4% after 2 years of injection up to 7% after 8 years of injection. The reduction of water cut by induced skin yields the reduction of the amount of injected water for the same volume of produced oil (Fig. 9). The effect of induced skin is more pronounced for the case of a volatile oil – the amount of injected clean water after 10 years of injection is 1.5 times higher than that for poor quality water causing $S=60$. The effect is weaker for the case of conventional oil: the amount of injected clean water is 1.3 times

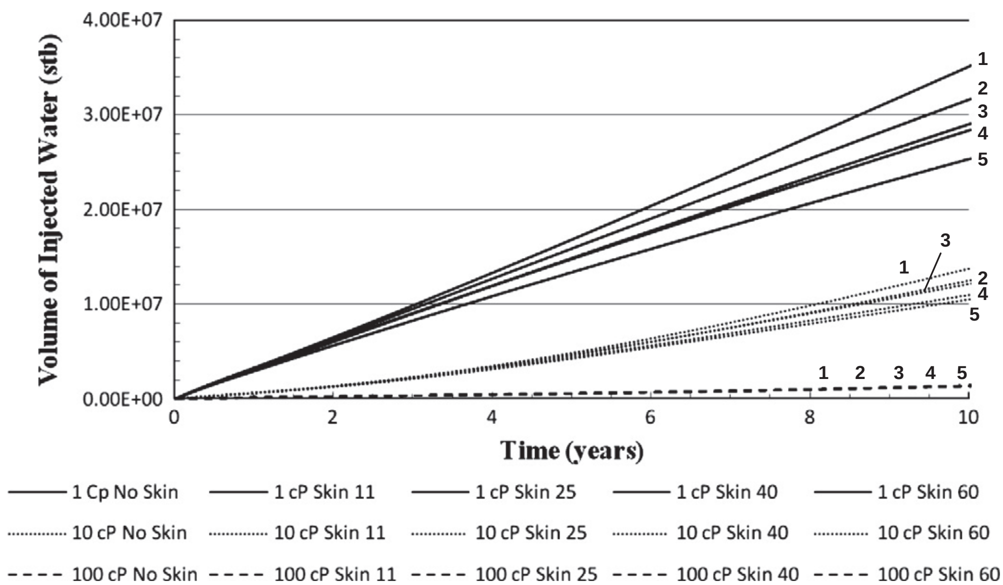

Fig. 9. Volume of injected water versus real time. Curves 1, 2, 3, 4 and 5 correspond to injection of clean water and of suspensions resulting in skin factors 11, 25, 40 and 60 after 10 years, respectively. Solid, dotted and dashed curves correspond to oil viscosities 1 cp, 10 cp and 100 cp, respectively.

higher than for the poor quality water. The effect almost disappeared for heavy oils – dashed curves 1, 2, 3, 4 and 5 in Fig. 9 almost coincide.

Finally, the main advantage of the induced homogenisation of the injectivity profile is the reduction of the volume of injected water for the same amount of produced oil. Since the balance of injected and produced fluids is maintained during the waterflood cases under consideration, the absolute reduction in injected water is equal to that in produced water under the same amount of produced oil. Like in the polymer flooding, the physics effect of improved recovery during injection of water with particles is the decreasing of water flux in swept zones. So, the IOR effects are also similar: the decreased amount of injected and produced water and some recovery increase after a long injection period (Lake, 1989).

An increase in horizontal well length makes the enhanced sweep effect more visible (injector and producer in Fig. 10 are 320 m long). It can be seen that the reservoir sweep in Fig. 10 is higher than that in Fig. 4. The following data were used: reservoir porosity $\phi = 0.3$, permeabilities of high and low permeable units are $k_h = 1.0$ d and $k_l = 0.05$ d, respectively, particle concentration $c^0 = 2.0$ ppm, filtration coefficient $\lambda^{/} = 1$ 1/m, formation damage coefficient $\beta = 1000$, critical porosity fraction determining the final skin due to particle dislodging $\alpha = 0.1$, cake porosity $\phi_c = 0.15$, cake permeability $k_c = 0.5$ md, well radius is $r_w = 0.1$ m. Those are typical values for damaged injectors (Bedrikovetsky et al., 2001; Moghadasi et al., 2004). Oil and water viscosities are 10 and 1 cp, respectively. Reservoir width, length and thickness are 600 m, 600 m and 20 m, respectively; inter-well distance is 442 m. The values of $\lambda^{/}$, β and α are the same for two zones, i.e. the effects of permeability on filtration parameters are ignored.

Figs. 10a,c,e shows areal saturation distribution during injection of suspension, while Fig. 10b,d,f illustrates water injection without skin. Fig. 10a,b presents saturation distributions in the reservoir after 0.3 PVI; Figs. 1c and 10d show saturation distribution after 1 PVI while Fig. 10e,f shows saturation field after 2 PVI. The main effect is the partial redirection of injected water into the low permeable zone due to high induced skin at the horizontal well section in the high permeability zone. A minor effect of sweep increase due to induced skin at the beginning of water injection (0.3 PVI) was observed. One can see the higher sweep in low permeability zone and the water saturation decrease in highly permeable area if compared with that of clean water flood at 1 PVI. The significant increase of sweep in low permeability zone after 2 PVI is apparent. In terms of the overall recovery, the incremental recovery factor increases up to 5% at 1 PVI and up to 9% after 2 PVI.

The dynamics of displacement presented in Fig. 10 allows comparing the effect of induced injectivity damage on incremental recovery for vertical and horizontal wells. For the case of vertical injector in thin two-layer-cake reservoir, the injected water bypasses the damaged zone near to the vertical injector by moving vertically along a short distance from low permeability to high permeability layer and enters the high velocity path. Almost all incremental flux in low permeability layer, induced by high skin in the high permeability layer, enters the high permeability layer. Distribution of fluxes along the layers remains the same downstream of the damaged area. It diminishes the effect of inhomogeneous skin profile on the waterflood sweep efficiency. Fig. 10 exhibits the case where the distance between wells has the same order of magnitude to the inter-zone distance. As in the thin two-layer-cake reservoir, the induced skin creates an additional resistance to flow in the high permeability zone and leads to an additional water flux entering the low permeability zone. Since the inter-zone distance is significantly higher than the distance between the high permeability and low permeability layers, the pressure gradient across the boundary is significantly lower in 2-zone reservoir. It allows for incremental flux in low permeable zone, caused by the injection rate redistribution due to the induced skin, to not fully move into highly permeable zone but displace more oil from the low permeability zone.

Let us consider the most favourable reservoir conditions of the application of waterflood with poor quality water. The recovery factor after 1 PVI is plotted against permeability ratio k_l/k_h (Fig. 11a) where the high permeability is 1 d, in which k_l and k_h are permeabilities of low and high permeability zones, respectively. As expected, the curve that corresponds to 'clean' waterflooding lies below than that for poor quality waterflood. If $k_l/k_h = 0$, oil is not recovered from the low permeability zone; sweep becomes equal for both cases of clean and poor quality water injection, which means that the incremental recovery vanishes. If $k_l/k_h = 1$, water displaces oil uniformly in both patterns, i.e. the displacement profile is already uniform, and the damage does not contribute to the straightening of the injectivity profile. This also means that the incremental recovery in homogeneous reservoirs is zero. So, two curves intercept at two points, and one curve is above the other in the interval between the two points (Fig. 11a). Therefore, there does exist a maximum point, where the incremental recovery is highest for some permeability ratio (Fig. 11b). The optimal

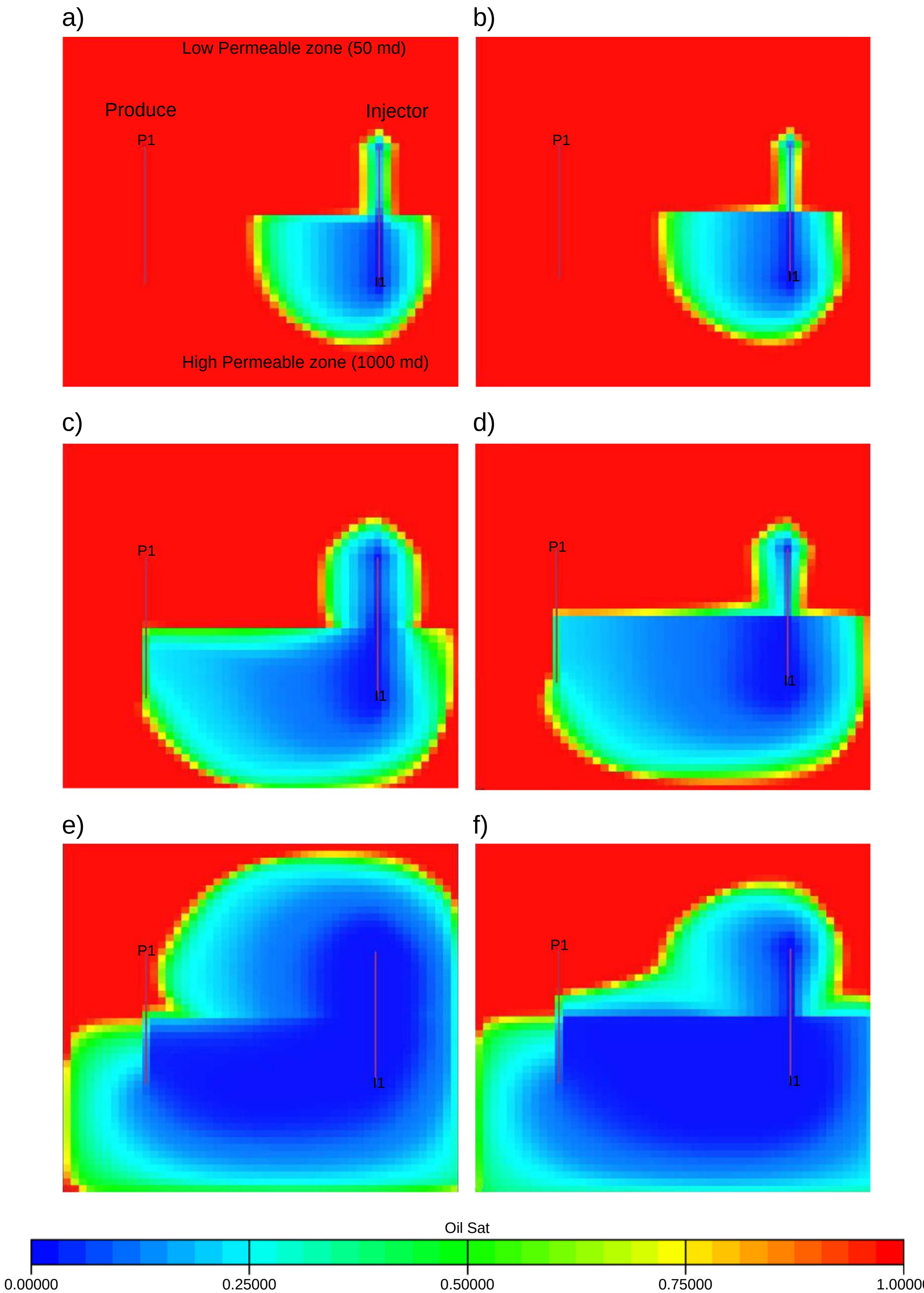

Fig. 10. Sweep efficiency increase due to skin factor distributed along the horizontal injector; the case of "long" horizontal well. a) Skin 60 at 0.3 PVI. b) No skin at 0.3 PVI. c) Skin 60 at 1 PVI. d) No skin at 1 PVI. e) Skin 60 at 2 PVI. f) No skin at 2 PVI.

permeability ratio is 0.05 for the case under consideration. For this case, the incremental recovery reaches the value 5% after 1 PVI and 9% after 2 PVI.

The waterflooding in two-zone reservoir was modelled using fine, moderate and coarse grids (grid parameters are presented in Table 1). For the case under consideration, the difference in

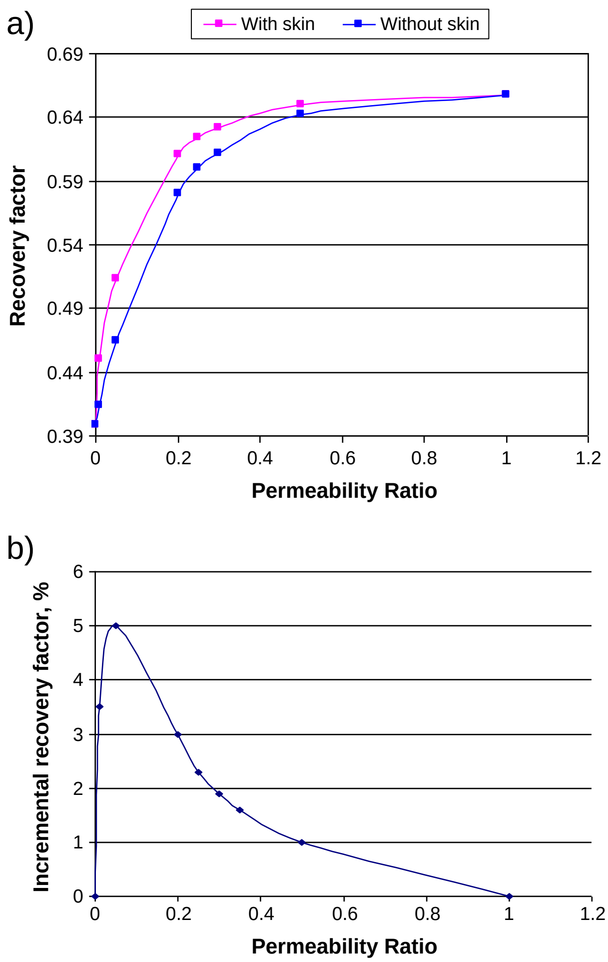

Fig. 11. Existence of the "optimal" permeability ratio k_l/k_h where the incremental recovery reaches its maximum: a) recovery factor during waterflood by clean water and suspension after 1 PVI as a function of permeability ratio; b) incremental recovery during waterflood by suspension if compared with clean water injection as a function of the permeability ratio.

simulation results with different size grids is negligible. Thus, the moderate grids are used for the simulated models.

5.2. Effect of induced injectivity skin on waterflooding in thin homogeneous reservoir with high permeability channel

Let us investigate the effect of skin, non-uniformly distributed along the horizontal injector, on waterflooding in the reservoir with high permeability channel. Fast breakthrough occurs via the channel, and it is interesting to find out whether the blocking of the entrance to the channel would prevent the fast water advance.

Two cases of quasi two-dimensional waterflood in a homogeneous reservoir with and without thin highly permeable channel, bridging the horizontal injector and producer, have been modelled, and the cases of injection of clean and particulated water have been compared. The recovery factors after injection of 1 PV of clean water in channelled and homogeneous reservoirs are 9% and 18%, respectively. The expected effect of suspension injection was the permeability decrease in the channel and, consequently, lower water cut and increased sweep efficiency. However, the simulation reveals some sweep increase only after a long injection period. The incremental recovery in the channelled reservoir after injection of 1 PVI is only 0.012, if compared with the clean water injection. The water cut reduction reaches 0.04 after a long period of 800 days of injection. This was explained by particle retention in the channel mostly near to the injector, so the injected water bypasses the small damage zone and enters the undamaged channel, which finally results in a low incremental recovery.

5.3. Bottom-up water injection using horizontal wells

Let us evaluate the effect of injectivity profile homogenization by the skin, induced by utilising poor quality water, for bottom-up injection in the system of horizontal injector and producer. The homogeneous rectangular reservoir was waterflooded by a horizontal injector below the horizontal producer (Fig. 12). The geometrical placement of wells in the reservoir is symmetrical with respect to planes x = 500 m and y = 500 m. The corresponding reservoir and formation damage properties are given in Tables 1 and 3. The constant pressures along both wells are assumed, i.e. the pressure losses due to fluid flows in well columns are neglected.

The speed along the shortest stream line AB in Fig. 12 highly exceeds those along the stream lines between the well heels and toes (curves CD and FE, respectively) that pass the remote areas near to the rectangular vortexes. This explains the poor sweep in periphery areas (Bedrikovetsky, 1993). The plugging by poor quality water occurs preferentially along the streamlines with higher speed, where the larger volumes of injected particles yield the higher particle retention concentrations. This occurrence constitutes to a natural conformance control by diverting the fluid from the zones, swept by high speed streamlines, to low speed zones which results in more uniform displacement of oil (enhanced sweep). In the case of two-zone reservoir, the effect of different speed along the streamlines was due to the heterogeneity of the reservoir, while in the bottom-up injection case it is due to the more complex geometry of stream lines.

The competitive factors of the improved sweep due to the redirection of water flux into the peripheral areas and of the reduced flux due to induced skin are the same as that in the two-permeability-zone reservoir. Yet, the gravity brings the additional complexity to the displacement process. The higher is the flow velocity in the gravity stable displacement the lower is the recovery (Lake, 1989; Bedrikovetsky, 1993). Plugging the high speed stream lines causes the recovery increase while the flow acceleration in low speed streamlines yields the decrease of the recovery factor. The complex interaction of the above gravity effects with the skin induced factors can be revealed by 3d numerical simulation.

The recovery factor versus time in PVI is presented in Fig. 13 for the injection of clean water and four cases of suspension injection. For the case of high skin S = 60, the incremental recovery factors for volatile,

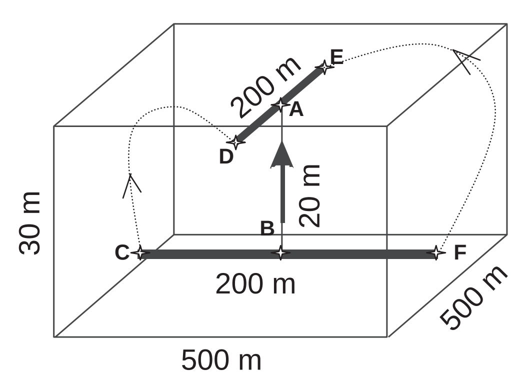

Fig. 12. Bottom-up water injection using horizontal wells. Dotted curves are streamlines CD and FE.

Table 3
Data for simulation of waterflooding in the bottom-up flooding study.

Data	S = 11	S = 25	S = 40	S = 60
λ' (1/m)	1	1	1	1
α	0.1	0.1	0.1	0.1
β	5	150	220	450
ϕ	0.3	0.3	0.3	0.3
c^0 (ppm)	5	10	10	15
r_w (m)	0.14	0.14	0.14	0.14
k_c (md)	20	20	20	20
ϕ_c	0.2	0.2	0.2	0.2

conventional and heavy oils after 1 PVI are 1.13%, 0.58% and 0.51%, respectively. Since the absolute recovery factors after 1 PVI are 24.34%, 12.29% and 5.62%, the ratios between the incremental recovery factors and the absolute recovery factors are 0.046, 0.047 and 0.090. Despite the incremental recovery factor decreases with increase of oil viscosity, the relative incremental recovery increases.

Fig. 14 presents the recovery factor *vs* real time for three cases of different viscosity oils and four skin values along with clean water flooding. The lower is the skin factor the higher is the recovery. The induction of skin due to poor quality water flooding (S = 60) results in decreasing of the recovery factor after 2 years of injection by 7.16% for volatile oil, by 1.49% for conventional oil and by 0.27% for heavy oil. Yet, the induced skin, that homogenizes the injectivity profile, causes the water cut to decrease (Fig. 15). The water cut decrease, if compared between the clean water injection and injection of poor quality water resulting in skin S = 60, for volatile oil is 13% for 5 months injection and 7.5% for 3-year injection. The water cut reduction decreases for more viscous oils. For the case of heavy oil, the water cut decrease is 8% for 5 months injection and 4.4% for 3 years of injection.

The effect of water cut reduction yields the significant reduction of injected and produced water volumes (Fig. 16). The injected water volume after 10-year injection is decreased by injection of poor quality water by 2.5 times for volatile oil, 2 times for conventional oils and 2.13 times for heavy oils.

6. Summary and discussion

The skin factor in injection wells due to the injection of particulated water monotonically increases with time. The analytical model provides explicit formulae for skin factor versus injected water volume. The option of water injection with a constant skin factor is already available in most black-oil simulators. Periodical recalculation of accumulated skin after injection of equal volumes using the analytical model allows for implementation of the injectivity decline model into a reservoir simulator for waterflooding. The ECLIPSE 100 black-oil reservoir simulator with implemented option of injectivity decline was applied for study of the effect of poorly treated water injection on sweep efficiency during waterflooding.

The injection of raw water causes formation injectivity damage due to the capture of particles by rock and the external filter cake formation. The damage results in a more uniform injectivity profile along the horizontal well. This continuous homogenisation of the injectivity profile during waterflooding yields the redirection of some injected water from the more permeable (higher swept) zones into the low permeable (lower swept) zones. The induced injection skin with waterflooding yields a reduced water-cut if compared with “clean” water injection – the water cut reduction occurs soon after the water breakthrough and remains up to 7–13% during a significant part

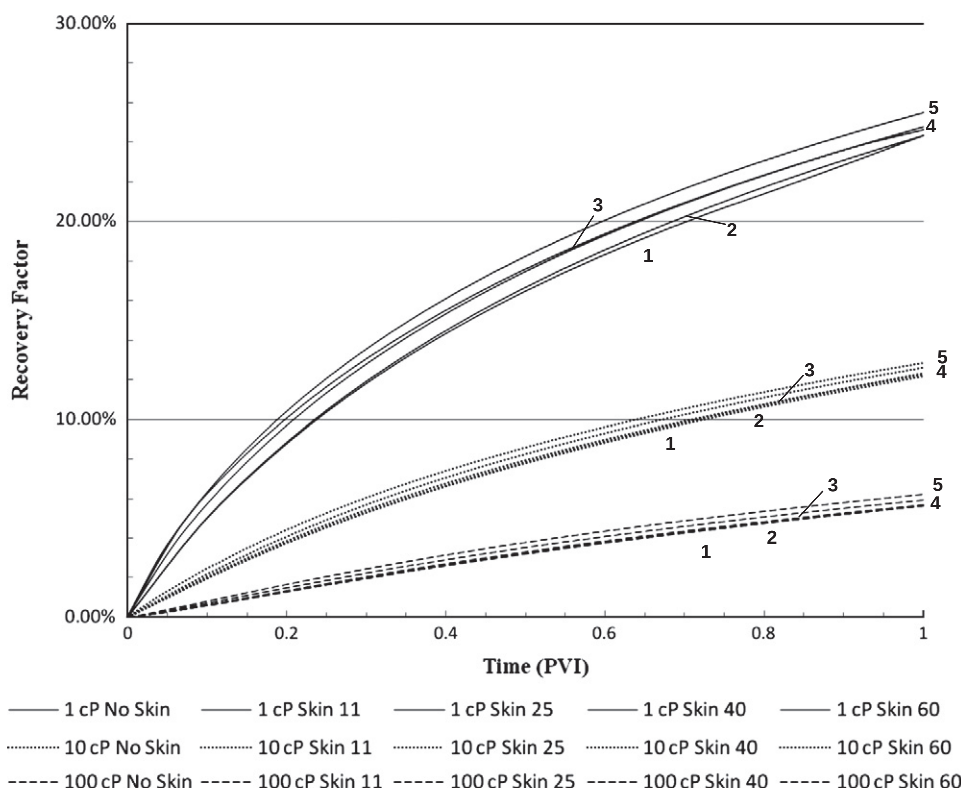

Fig. 13. Comparison of recovery factors versus PVI for injection of suspension and of “clean” water. Curves 1, 2, 3, 4 and 5 correspond to injection of clean water and of suspensions resulting in skin factors 11, 25, 40 and 60 after 1 PVI, respectively. Solid, dotted and dashed curves correspond to oil viscosities 1 cp, 10 cp and 100 cp, respectively.

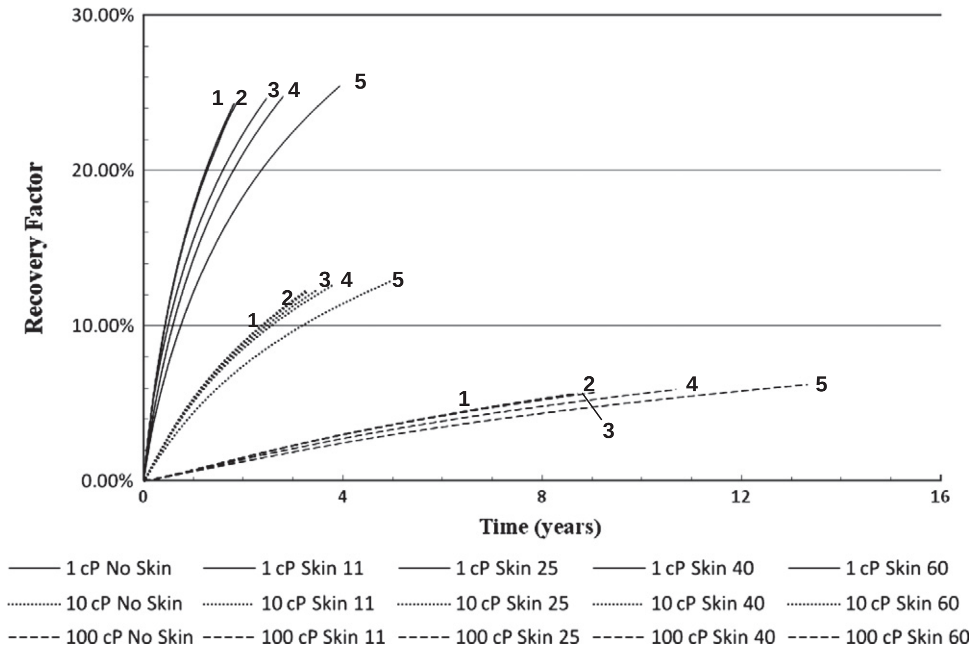

Fig. 14. Recovery factor vs real time (years) for Oil Viscosity of 1 cp, 10 cp and 100 cp after 1 PVI. Curves 1, 2, 3, 4 and 5 correspond to injection of clean water and of suspensions resulting in skin factors 11, 25, 40 and 60 after 1 PVI, respectively. Solid, dotted and dashed curves correspond to oil viscosities 1 cp, 10 cp and 100 cp, respectively.

of the production period. So, the water cut is lower for the case of raw water injection. It also results in some sweep increase. Yet, the induced skin results in some delay in reaching the given recovery factor if compared with the injection of 'clean' water due to production and injection rates reduction.

The above effects are more pronounced for volatile oils and can be relatively small for heavy oils.

The effects of water cut reduction and delayed IOR for raw water injection are similar to those of polymer flooding, since both technologies result in decrease of the injected water mobility.

The main positive effect of waterflooding with raw water, causing a decrease of injectivity index, is the economic benefit due to savings on injected water treatment. The latter is applied for poorly treated seawater injection as well as for the re-injection of produced water. The advantage of savings on water treatment is especially important for off-shore waterfloods, where the limited and expensive space in platforms yields a high cost of water treatment. Another important advantage is savings due to reduction of injected and produced waters. The disadvantage is the total production rate reduction due to the induced skin factor, which may cause some reduction in oil production rate. This disadvantage is negligible for waterflooding in two-permeability-zone reservoir, where the effect of decreased water cut compensates the effect of the total rate decrease. Yet, some reduction in oil production was observed for bottom-up waterflooding. The final decision on utilising this method must be made after performing the quantitative economic analysis, which is outside the scope of this work.

The above conclusions are valid for the idealised reservoir model adopted in this work: the reservoir pressure does not rise to the level of the fracturing pressure, deformation and geo-mechanics effects are negligible, simple two-zone heterogeneity was considered. The application of the poor quality water injection in concrete oilfields requires more complex reservoir model and economic analysis.

It is expected that the application of poor quality aqueous suspension may also result in a reduction of water cut and an increase of sweep efficiency for extended fractured injectors and for different configurations of horizontal and slanted wells (see Bachman et al., 2003).

7. Conclusions

The analytical model for injectivity impairment due to poor quality injected water can be implemented in black oil reservoir simulator. Simulation of lateral waterflooding in two-permeability-zone reservoir and of bottom-up flood in a homogeneous reservoir with horizontal injector and producer allows the following conclusions to be drawn:

(1) Injection of poor quality water results in in-homogeneously distributed skin factor as the skin varies along the well according to the injection rate variation;
(2) The induced skin yields a partial homogenization of the injectivity profile;
(3) Poor quality water injection results in significant reduction of injected and produced water if compared with the clean water flooding and in some increase of sweep efficiency while causing the total production rate reduction;
(4) The negative effect of the total rate reduction is compensated by the positive effect of water cut reduction for lateral flood of a two-permeability-zone reservoir where the induced skin does not affect the oil production history;
(5) The induced skin causes some reduction in oil production rate for bottom-up flooding;
(6) The incremental recovery factor is higher for lower viscosity oils. Yet, the ratio between the incremental recovery factor and the recovery factor after 1 PVI increases with increasing oil viscosity;
(7) The feasibility of poor quality water flooding is a subject to detailed economic analysis.

Acknowledgements

The authors thank Petrobras for the generous sponsorship of the injectivity damage project over many years. Many thanks are due to Australian School of Petroleum, University of Adelaide and Schlumberger Australia for encouraging and supporting this work.

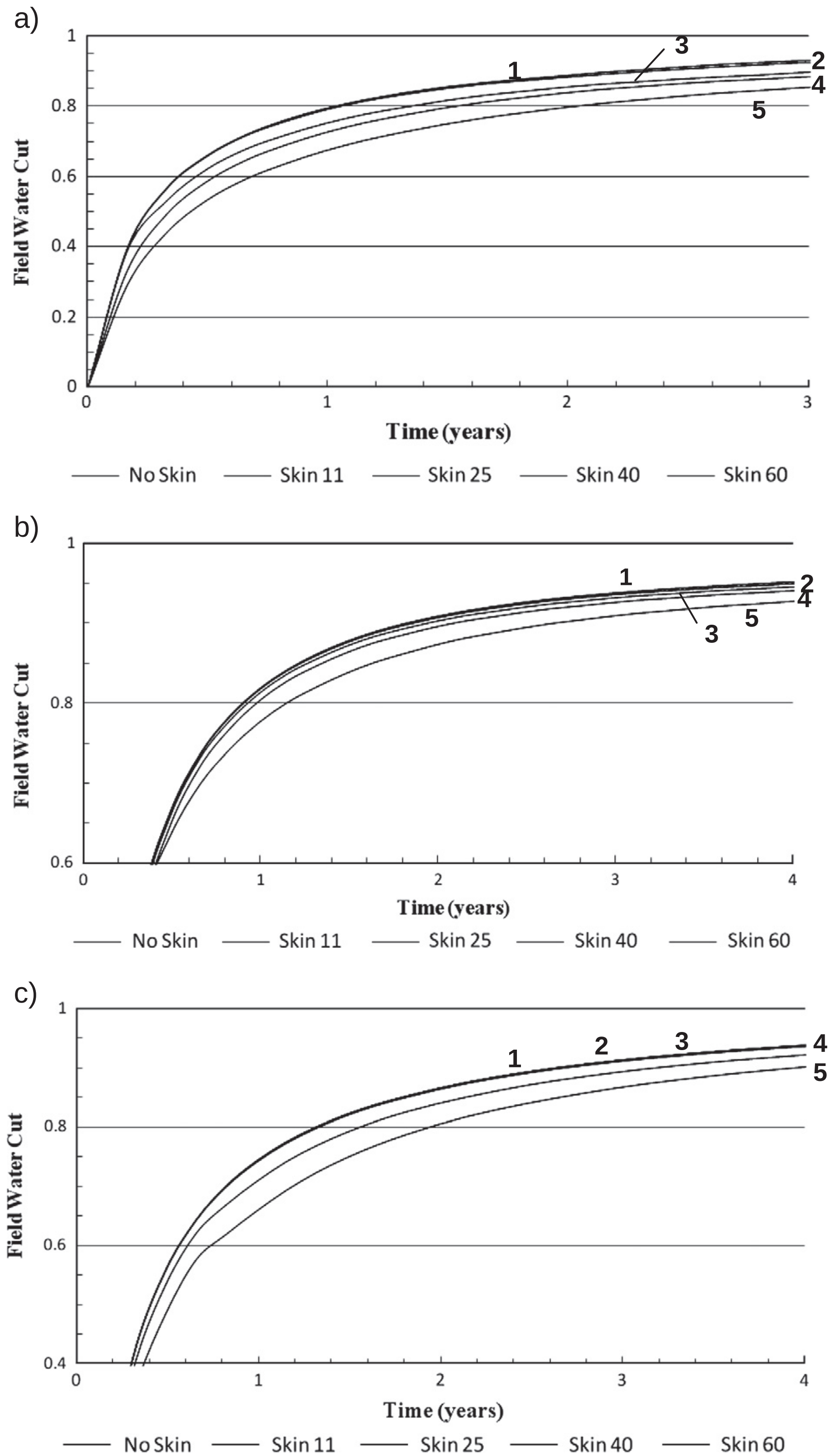

Fig. 15. Water cut during injection of suspension and of clean water, versus real time. Curves 1, 2, 3, 4 and 5 correspond to injection of clean water and of suspensions resulting in skin factors 11, 25, 40 and 60 after 1 PVI, respectively. a) oil viscosity is 1 cp, b) oil viscosity is 10 cp, c) oil viscosity is 100 cp.

Appendix A. Analytical model for injectivity damage due to injection of poor quality water

The analytical model for injectivity decline due to the injection of suspended aqueous colloids contains explicit formulae for suspended and retained particle concentrations, pressure drop and rate and well index versus time (Herzig et al., 1970; Nabzar et al., 1997; Pang and Sharma, 1997; Wennberg and Sharma, 1997; Ochi et al., 1999; Bedrikovetsky et al., 2005; Paiva et al., 2007). Here we present the formulae for skin factor growth with time.

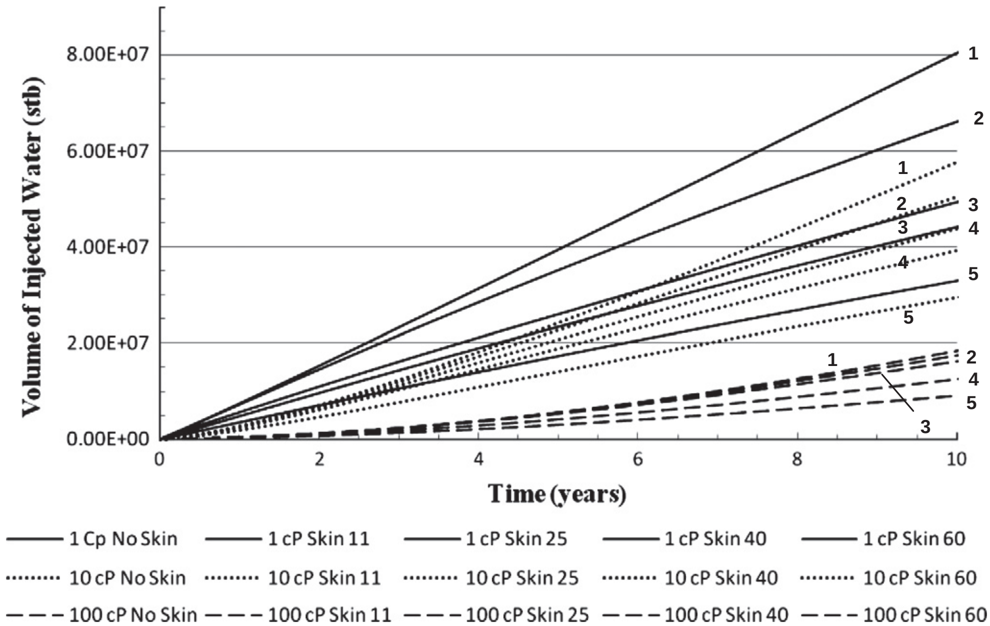

Fig. 16. Volume of injected water versus real time. Curves 1, 2, 3, 4 and 5 correspond to injection of clean water and of suspensions resulting in skin factors 11, 25, 40 and 60 after 1 PVI, respectively. Solid, dotted and dashed curves correspond to oil viscosities 1 cp, 10 cp and 100 cp, respectively.

Skin grows linearly with time during deep bed filtration

$$S = m\ln {}^{r_e}\!/_{r_w}\, t_D$$
$$m(\lambda',\beta)=\frac{\beta\phi c^0(\lambda' r_w)^2}{2}\left(\frac{1}{\lambda' r_w}+e^{\lambda' r_w}\mathrm{ei}(\lambda' r_w)\right) \qquad (A-1)$$
$$t_D=\frac{qt}{\pi\phi r_e^2 h}$$

where t_D is dimensionless time calculated in PVI.

The dimensionless transition time in PVI, when the particle percolation into reservoir comes to the limit, is

$$t_{Dtr}=\frac{2\alpha r_w}{\lambda' r_e^2 c^0} \qquad (A-2)$$

where α is the critical porosity fraction showing at which retention concentration particles do not penetrate into the reservoir any more (Pang and Sharma, 1997).

During the external filter cake formation, skin factor is also a linear function of dimensionless time

$$S = \ln {}^{r_e}\!/_{r_w}\left(m t_{Dtr}+m_c(t_D-t_{Dtr})\right)$$
$$m_c=\frac{k_0 k_{rwor}\phi\ c^0}{2k_c(1-\phi_c)X_w(-\ln X_w)},\ X_w=\left(\frac{r_w}{r_e}\right)^2 \qquad (A-3)$$

Here X_w is the dimensionless well radius.

The dependence (A-3) holds until the erosion time t_e (Fig. 3).

Appendix B. Cake erosion

Let us calculate the thickness of the external filter cake where the moments of drag, electrostatic and permeate forces are equal, as proposed in the literature (Jiao and Sharma, 1994; Freitas and Sharma, 2001).

Drag force (F_d) acting on a small spherical particle in a cylindrical tube is derived from asymptotic solution of the Navier-Stokes equations (Al-Abduwani et al., 2005b)

$$F_d=\frac{36\mu a^2 Q_{cf}}{(r_w-h_c)^3} \qquad (B-1)$$

Here a is the injected particle diameter and Q_{cf} is the average cross-flow rate.

The permeate force (F_p) acting on a particle is derived from Stokes formula (Al-Abduwani et al., 2005b)

$$F_p=\frac{3\mu aq}{r_w-h_c} \qquad (B-2)$$

where q is the flow rate.

The drag force increases during cake build-up due to the decrease of well cross section accessible for flux. The pressure drop between the well wall and the reservoir remains constant during growth of the external filter cake, so the pressure gradient across the cake decreases. Thus, the permeate force exerting the particle on the cake surface decreases.

Another force "sticking" the particle to the cake surface is the electrostatic DLVO force that varies along the particle-cake separation distance. Since the critical cake thickness corresponds to mechanical equilibrium of particles on the cake surface and further dislodging, the maximum value of electrostatic force F_e enters into the force (torque) balance.

Particle deposition on the cake surface stops when the total torque (moment) of drag, electrostatic and permeate forces becomes zero, i.e.

$$F_p+F_e=\ E_r\sqrt{3}F_d \qquad (B-3)$$

where F_e is the electrostatic force and the erosion factor is $E_R=0.03$ (Paiva et al., 2007).

We assume constant pressure drop between the well and the reservoir along the well, i.e. the injection rate q is constant along the well. Therefore, average cross flow rate Q_{cf} is equal to half of overall injected rate qL, where L as the well length.

All injected particles deposit on the cake surface, allowing for the following expression for the cake thickness h_c

$$h_c(t) = \frac{c^o}{2\pi r_w(1-\phi_c)} \int_{t_{tr}}^{t} q(t)dt \qquad (B-4)$$

Substituting of expressions for drag and permeate forces Eq. (B-1, 2) into equality of force moment balance in Eq. (B-3) and neglecting the electrostatic force yields the critical cake thickness

$$h_{cr} = r_w - \sqrt{E_r\sqrt{3}*6aL} = r_w - \sqrt{0.3aL} \qquad (B-5)$$

Formula (B-5) shows that the value 0.3aL is less than r_w^2 if cake thickness is positive. The opposite means that the particles are large enough for drag force to sweep away all the particles from the well wall.

From Eq. (B-4) follows the equation for time of cake erosion t_e

$$\frac{c^o}{2\pi r_w(1-\phi_c)} \int_{t_{tr}}^{t_e} q(t)dt = \left(r_w - 0.51\sqrt{aL}\right) \qquad (B-6)$$

References

Al-Abduwani, F.A.H., Shirzadi, A., Van Den Broek, W.M.G.T., Currie, P.K., 2005a. Formation damage *vs*. solid particles deposition profile during laboratory-simulated produced-water reinjection. SPE Paper 82235: SPE Journal, 10 (2), pp. 138–151. June.

Al-Abduwani, F., Bedrikovetsky, P., Farajzadeh, R., van den Broek, W.M.G.T., Currie, P.K., 2005b. External filter cake erosion: mathematical model and experimental study. SPE Paper 94635 presented at the SPE 6th European Formation Damage Conference, Scheveningen, The Netherlands. 25-27May.

Ali, M.A.J., Currie, P.K., 2007. Permeability damage due to water injection containing oil droplets and solid particles at residual oil saturation. SPE Paper 104608 presented at the SPE Middle East Oil and Gas Show and Conference, Kingdom of Bahrain. 11-14 March.

Ali, M.A.J., Currie, P.K., Salman, M.J., 2005. Measurement of the particle deposition profile in deep-bed filtration during produced water re-injection. SPE Paper 93056 presented at the SPE Middle East Oil and Gas Show and Conference, Kingdom of Bahrain. March 12-15.

Aziz, K., Settari, A., 2002. Petroleum Reservoir Simulation. Blitzprint, Calgary, Alberta, Canada.

Bachman, R.C., Harding, T.G., Settari, A., Walters, D.A., 2003. Coupled simulation of reservoir flow, geomechanics, and formation plugging with application to high-rate produced-water reinjection. SPE Paper 79695 presented at the SPE Reservoir Simulation Symposium, Huston, Texas, USA. 03-05-Feb.

Bedrikovetsky, P.G., 1993. Mathematical theory of oil and gas recovery (with applications to the development of the ex-USSR oil and gas-condensate reservoirs). Kluwer Academic Publishers, London/Boston/Dordrech.

Bedrikovetsky, P., 2008. Upscaling of stochastic micro model for suspension transport in porous media. J. Trans. Por. Media 75 (3), 335–369.

Bedrikovetsky, P.G., Marchesin, D., Shecaira, F., Serra, A.L., Resende, E., 2001. Characterization of deep bed filtration system from laboratory pressure drop measurements. J.Petrol. Sci. Eng. 64 (3), 167–177.

Bedrikovetsky, P., Da Silva, M.J., Da Silva, M.F., Siqueira, A.G., De Souza, A.L.S., Furtado, C., 2005. Well-history-based prediction of injectivity decline during seawater flooding. SPE Paper 93886 presented at the SPE 6th European Formation Damage Conference, Scheveningen, The Netherlands, May 25–27.

Bennion, D.B., Thomas, F.B., Bietz, R.F., 1996. Formation damage and horizontal wells – a productivity killer? SPE Paper 37138 presented at the SPE International Conference on Horizontal Well Technology, 18–20 November.

Chauveteau, G., Nabzar, L., Coste, J.-P., 1998. Physics and modelling of permeability damage induced by particle deposition. SPE Paper 39463 presented at the SPE Formation Damage Control Conference, Lafayette, Louisiana, USA, 18–19 February.

Civan, F., 2007. Reservoir formation damage, fundamentals, modeling, assessment, and mitigation, 2nd ed. Gulf Publishing Company, Houston, U.S.A.

Das, O.P., Aslam, M., Bahuguna, R., Khalaf, A.-E., Al-Shatti, M., Yousef, A.-R.T., 2009. Water injection monitoring techniques for minagish oolite reservoir in west Kuwait. SPE Paper 13361 presented at the International Petroleum Technology Conference, Doha, Qatar, 7–9 December 2009.

Freitas, M., Sharma, M., 2001. Detachment of particles from surfaces: an afm study. J. Colloidal Int. Sci. 233 (1), 73–82.

Furtado, C.J.A., Souza, A.L.S., Araujo, C.H.V., 2007. Evaluation of different models for injectivity decline prediction. SPE Paper 108055 presented at Latin American & Caribbean Petroleum Engineering Conference, Buenos Aires, Argentina.

Furui, K., Zhu, D., Hill, A.D., 2003. A rigorous formation damage skin factor and reservoir inflow model for a horizontal well (includes associated papers 88817 and 88818) SPE Paper 84964, J. SPE P&F. 18 (3), 151–157.

Herzig, J.P., Leclerc, D.M., Le Goff, P., 1970. Flow of suspensions through porous media—application to deep filtration. Ind. Eng. Chem. 62 (5), 8–35.

Hoek van den, P.J., 2004. Impact of induced fractures on sweep and reservoir management in pattern floods. SPE Paper 90968 presented at the SPE Annual Technical Conference and Exhibition, Houston, Texas. 26–29 September 2004.

Izgec, B., Kabir, C.S., 2009. Real-time performance analysis of water-injection wells SPE Paper 109876 J SPE REE. 12 (1), 116–123.

Jiao, D. And, Sharma, M., 1994. Mechanism of cake build-up in cross-flow filtration of colloidal suspensions. J. Colloidal Int. Sci. 162 (2), 454–462.

Khambharatana, F., Thomas, S., Ali, S.M., Farouq, 1997. Numerical simulation and experimental verification of oil recovery by macroemulsion floods. SPE Paper 39033 presented at the Latin American And Caribbean Petroleum Engineering Conference, Rio De Janeiro, Brazil. 30 August-3 September 1997.

Khambharatana, F., Thomas, S., Ali, S.M., Farouq, 1998. Macroemulsion rheology and drop capture mechanism during flow in porous media. SPE 48910 presented at the SPE International Oil And Gas Conference And Exhibition, Beijing, China. 2–6 November.

Lake, L.W., 1989. Enhanced Oil Recovery. Prentice Hall, Engelwood Cliffs, NY.

Moghadasi, J., Müller-Steinhagen, H., Jamialahmadi, M., Sharif, A., 2004. Theoretical and experimental study of particle movement and deposition in porous media during water injection. J. Petrol. Sci. Eng. 43 (3–4), 163–181.

Mojarad, R.S., Settari, A., 2007. Coupled numerical modelling of reservoir flow with formation plugging. J. Can. Pet. Technol. 46 (3), 54–59.

Nabzar, L., Chauveteau, G., Roque, C., 1996. A new model for formation damage by particle retention. SPE Paper 311190 presented at the SPE Formation Damage Control Conference, Lafayette, Louisiana. 14–15 February.

Nabzar, L., Coste, J.P., Chauveteau, G., 1997. Water quality and well injectivity. Paper 044 presented at the 9th European Symposium On Improved Oil Recovery, The Hague, The Netherlands.

Nunes, M., Bedrikovetsky, P., Newbery, B., Furtado, C.A., Souza, A.L., 2010. Theoretical definition of formation damage zone with applications to well stimulation. J. Energy Res. Technol. 132 (3) 033101-1-7.

Ochi, J., Detienne, J.L., Rivet, P., Lacourie, Y., 1999. External filter cake properties during injection of produced water. SPE Paper 54773 presented at the SPE European Formation Damage Conference, The Hague, Netherlands. 31 May-1 June 1999.

Ojukwu, K.I., Hoek van den, P.J., 2004. A new way to diagnose injectivity decline during fractured water injection by modifying conventional Hall analysis. SPE Paper 89376 presented at the SPE/DOE Symposium on Improved Oil Recovery, Tulsa, Oklahoma. 17–21 April 2004.

Paiva, R., Bedrikovetsky, P., Furtado, C.A., Siqueira, A., Souza, A.L., 2007. A comprehensive model for injectivity decline prediction during pwri (renewed version). SPE Paper 107866 to be presented at the European Formation Damage Conference held in Scheveningen, The Netherlands. 30 May–1 June 2007.

Pang, S., Sharma, M.M., 1997. A model for predicting injectivity decline in water-injection wells. SPEFE-28489, 12 (3, pp. 194–201.

Rousseau, D., Hadi, L., Nabzar, L., 2007. PWRI-induced injectivity decline: new insights on in-depth particle deposition mechanisms. SPE Paper 107666 presented at the SPE European Formation Damage Conference, Sheveningen, The Netherlands. 30-May/01-June.

Schlumberger Information Solutions (SIS), 2008. ECLIPSE reservoir engineering software Schlumberger Limited. Available Online http://www.Slb.Com/Content/Services/Software/Reseng/Index.Asp2008.

Shapiro, A., Bedrikovetsky, P., 2008. Elliptic random-walk equation for suspension and tracer transport in porous media. Phys. A: Stat. Mech. App. 387 (24), 5963–5978.

Sharma, M.M., Yortsos, Y.C., 1987. Transport of particulate suspensions in porous media: model formulation. Aiche J. 33 (10), 1636–1643.

Soo, H., Radke, C.J., 1986a. A filtration model for the flow of dilute, stable emulsions in porous media – I theory –. Chem. Eng. Sci. 41 (2), 263–272.

Soo, H., Radke, C.J., 1986b. A filtration model for the flow of dilute, stable emulsions in porous media – Ii parameter evaluation and estimation. Chem. Eng. Sci. 41 (2), 273–281.

Souza, A.L.S., Figueiredo, M.W., Kuchpil, C., Bezerra, M.C., Siqueira, A.G., Furtado, C.A., 2005. Water management in Petrobras: developments and challenges. OTC Paper 17258 presented at the 2005 Offshore Technology Conference held in Houston, TX, U.S.A. 2–5 May.

Wennberg, K.E., Sharma, M.M., 1997. Determination of the filtration coefficient and the transition time for water injection wells. SPE Paper 38181 presented at the SPE European Formation Damage Conference, The Hague, Netherlands. 2–3 June.

Glossary

a: Particle radius, L, μm
c: Suspended particle concentration, ppm
c^0: Injected suspended particle concentration, ppm
e: Exponential
ei: Error function
E_r: Erosion factor
F_d: Drag force, ML/T^2, N
F_e: Electrostatic force, ML/T^2, N
F_p: Permeate force, ML/T^2, N

h: Thickness of the reservoir, L, m
h_c: Cake thickness, L, m
h_{cr}: Critical cake thickness, L, m
j: Impedance, i.e. reciprocal normalised injectivity index
k: Absolute permeability of water, L^2, m^2
k_0: Original (formation/core) permeability before the injection, L^2, m^2
k_c: External cake permeability, L^2, m^2
k_l: Low permeability in 2-zone reservoir, L^2, m^2
k_h: High permeability in 2-zone reservoir, L^2, m^2
k_{rwor}: Relative permeability of water at residual oil
L: Well length, L, m
m: Slope of the impedance straight line during deep bed filtration
m_c: Slope of the impedance straight line during external cake formation
p: Pressure, M/LT^2, Pa
p_e: Average reservoir pressure, M/LT^2, Pa
p_w: Well pressure, M/LT^2, Pa
q: Total flow rate per unit of reservoir thickness, L^2/T, m^2/s
q_0: Initial flow rate per unit of reservoir thickness in undamaged well, L^2/T, m^2/s
Q_{cf}: Average cross-flow rate, L^3/T, m^3/s
r: Radius, L, m
r_e: Well drainage radius, L, m
r_w: Well radius, L, m
S: Skin factor
t: Time, T, s
t_D: Dimensionless time
t_{De}: Dimensionless erosion time
t_{Dtr}: Dimensionless transitions time
t_e: Erosion time, T, s
t_{tr}: Transitions time, T, s
X_w: Dimensionless well radius

Greek letters

α: Critical porosity fraction
β: Formation damage coefficient
Δp: Pressure drop, M/LT^2, Pa
Δp_0: Initial pressure drop in undamaged well, M/LT^2, Pa
λ': Filtration coefficient, L^{-1}, m^{-1}
μ: Viscosity, M/LT, Pa.s
μ_w: Water viscosity, M/LT, Pa.s
ϕ: Porosity
ϕ_c: External cake porosity
π: Pi